Activities of components in Ca_2SiO_4-$Ca_3P_2O_8$ solid solution at 1573 K

K Saito[1] and *M Hasegawa*[2]

1. Graduate Student, Kyoto University, Kyoto, Japan, 606-8501
   Email: saito.keijiro.x38@kyoto-u.jp
2. Associate Professor, Kyoto University, Kyoto, Japan, 606-8501
   Email: hasegawa.masakatsu.7r@kyoto-u.ac.jp

Keywords: dephosphorization, di-calcium silicate, tri-calcium phosphate, P_2O_5, activity

ABSTRACT

In steelmaking processes, it is known that P_2O_5 in dephosphorization slags often exists in solid solutions between Ca_2SiO_4 and $Ca_3P_2O_8$, $<C2S\text{-}C3P>_{SS}$, and thus the solid solutions play an important role in the dephosphorization reaction. Hence, the knowledge of thermochemical properties, ie, phase relations and activities of components, in slags containing $<C2S\text{-}C3P>_{SS}$ are necessary for the effective removal of phosphorus from hot metal. In this study, the P_2O_5 activities in $<C2S\text{-}C3P>_{SS}$ were measured through the gas equilibrium method.

In the present experiment, oxide samples were equilibrated with Cu-P liquid alloys at 1573 K under a stream of Ar + H_2 + H_2O or Ar + H_2 + CO_2 gas mixture in which oxygen potential was fixed, and then equilibrium phosphorus concentrations in the Cu-P alloys, $[mass\%P]_{Cu}$, were analysed with ICP-OES. The underlying reaction can be expressed by

$$2[P]_{Cu} + (5/2)O_2(gas) = P_2O_{5\ in\ oxide}$$

$$K = a_{P_2O_5}\,(p_{O_2}/atm)^{-5/2}\,[mass\%P]_{Cu}^{-2}$$

, where K denotes the equilibrium constant, $a_{P_2O_5}$ represents the P_2O_5 activity, and p_{O_2} is the oxygen partial pressure in the gas phase. Firstly, the experiments were performed on MgO + $Mg_3P_2O_8$, in which the P_2O_5 activity has already been reported, to determine the value for the equilibrium constant, K. Subsequently, the P_2O_5 activities were measured in $<C2S\text{-}C3P>_{SS}$ + $CaSiO_3$ and $<C2S\text{-}C3P>_{SS}$ + CaO with the same experimental procedure.

The P_2O_5 activity in $<C2S\text{-}C3P>_{SS}$ coexisting with CaO was found to be about seven digits lower than that with $CaSiO_3$ even at the same composition of $<C2S\text{-}C3P>_{SS}$. This phenomenon was explained in terms of the activities of Ca_2SiO_4 and $Ca_{1.5}PO_4$ (= (1/2)$Ca_3P_2O_8$). These activities are determined depending on temperature and the composition of $<C2S\text{-}C3P>_{SS}$, while the P_2O_5 activity depends not only on these variables but also on the second phase coexisting with $<C2S\text{-}C3P>_{SS}$. The Ca_2SiO_4 and $Ca_{1.5}PO_4$ activities exhibited large negative deviations from Raoult's law, which implied the strong chemical affinity between the components. Experimental errors in these experiments would be cancelled out in calculating $a_{P_2O_5}$ since they would be involved in both experimental procedures for MgO + $Mg_3P_2O_8$ and $<C2S\text{-}C3P>_{SS}$ + CaO or $<C2S\text{-}C3P>_{SS}$ + $CaSiO_3$, which makes the present results more reliable.

INTRODUCTION

Phosphorus is a typical harmful element in steel and is removed from molten iron by the following oxidation reaction in the steelmaking processes.

$$2[P]_{Fe} + 5FeO_{\ in\ slag} = P_2O_{5\ in\ slag} + 5Fe(liquid) \qquad (1)$$

$$\log K_1 = \log a_{P_2O_5} - 5\log a_{FeO} - 2\log([f_P]_{Fe}\,[mass\%P]_{Fe})$$

$$= 12730/(T/K) - 20.0 \qquad \text{(Hino and Ito, 2009)} \qquad (2)$$

, where $[P]_{Fe}$ and $[f_P]_{Fe}$ denote phosphorus in molten iron and its Henrian activity coefficient, respectively, while a_i represents the Raoultian activity of component i in the slag. The standard states of a_{P2O5} and a_{FeO} are taken to be pure hypothetical liquid P_2O_5 and pure liquid FeO in equilibrium with metallic iron, respectively. It is known that P_2O_5 reacts with CaO and SiO_2 in slags to form solid solutions between di-calcium silicate, Ca_2SiO_4, and tri-calcium phosphate, $Ca_3P_2O_8$. The phosphorus oxides are enriched in such solid solutions, and thus the solid solutions have an important role in the dephosphorization reaction (Kitamura, Shibata, and Maruoka, 2008). Figure 1 gives a part of the $CaO\text{-}SiO_2\text{-}P_2O_5$ ternary phase diagram at 1573 K (Matsu-suye *et al*, 2007; Uchida, Watanabe, and Hasegawa, 2021; Uchida, Watanabe, and Tsuruoka, 2022) and the $Ca_2SiO_4\text{-}Ca_3P_2O_8$ pseudo-binary phase diagram (Fix, Heymann and Heinke, 1969). It can be seen that the solid solution between α-Ca_2SiO_4 and $\acute{\alpha}$-$Ca_3P_2O_8$ can coexist with $CaSiO_3$ or CaO when the $Ca_3P_2O_8$ content is 10 - 40 mass% at 1573 K. In Figure 1 and hereafter, the following abbreviations are used.

$C2S$ = $2CaO{\cdot}SiO_2$ = Ca_2SiO_4
CS = $CaO{\cdot}SiO_2$ = $CaSiO_3$
$C3P$ = $3CaO{\cdot}P_2O_5$ = $Ca_3P_2O_8$

M3P = $3MgO \cdot P_2O_5$ = $Mg_3P_2O_8$
<*C2S-C3P*>$_{SS}$ = Ca_2SiO_4-$Ca_3P_2O_8$ solid solution

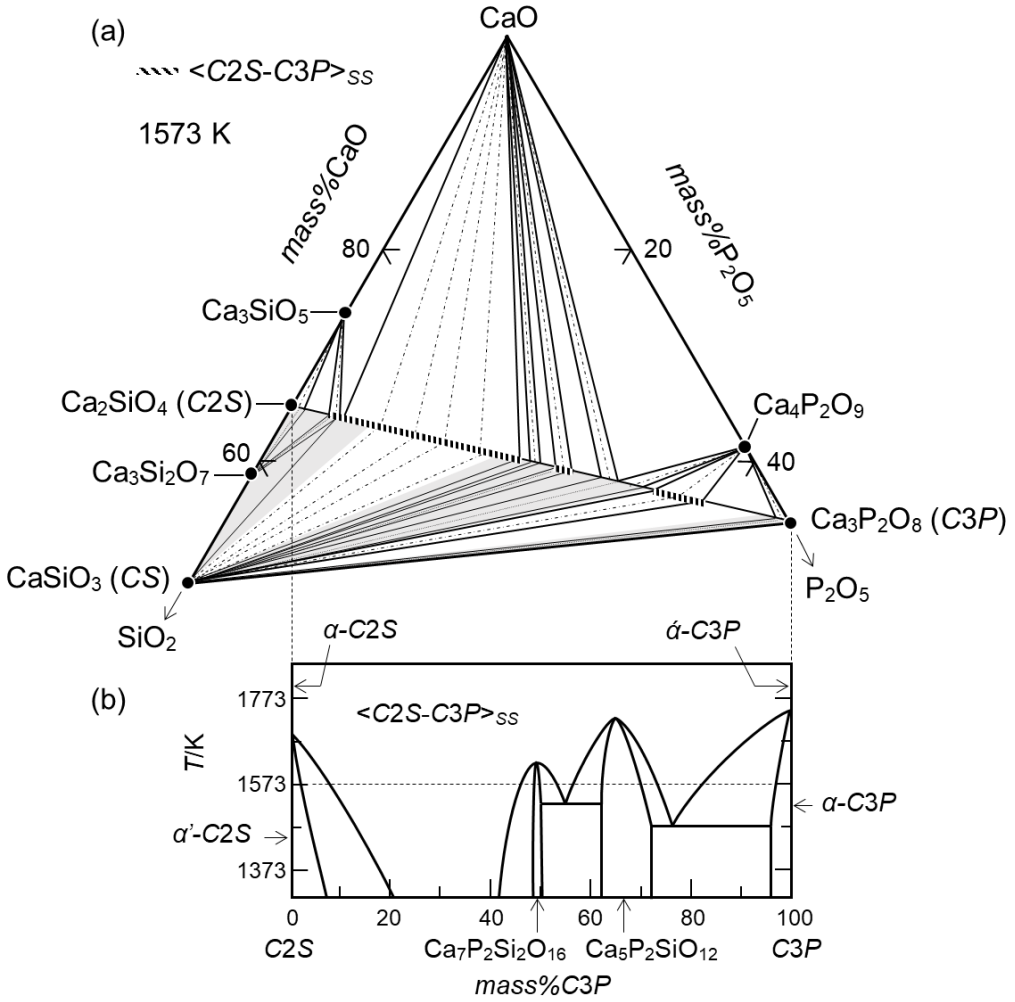

FIG 1a - CaO-SiO_2-P_2O_5 ternary phase diagram at 1573 K.
The grey-shaded areas are unknown and estimated.
b - Ca_2SiO_4-$Ca_3P_2O_8$ pseudo-binary phase diagram.

According to Le Chatelier's principle, Reaction (1) can proceed effectively in conditions of low temperature, high FeO activity, low P_2O_5 activity, and high P activity coefficient. If the molten iron is regarded as a carbon-saturated Fe-C-P liquid alloy, the Henrian activity coefficient of phosphorus, $[f_P]_{Fe}$, can be expressed by using interaction parameters, e_i^j.

$$\log[f_P]_{Fe} = e_P^C [mass\%C]_{Fe} + e_P^P [mass\%P]_{Fe}$$

$$= 0.126[mass\%C]_{Fe} + 0.054[mass\%P]_{Fe} \quad \text{(Hino and Ito, 2009)} \quad (3)$$

When iron ore is reduced by carbon, dissolving carbon in pig iron can decrease the liquidus temperature and increase $[f_P]_{Fe}$ in the iron alloy, which is advantageous to the phosphorus removal. On the other hand, concerning hydrogen reduction aiming at carbon-neutral refinings, phosphorus exists as an impurity also in hydrogen-reduced iron to the same extent as the carbon-reduced one (Kashiwaya and Hasegawa, 2012). The phosphorus content after dephosphorization from the carbon- or hydrogen-reduced molten iron can be compared as follows. The refining temperatures were assumed to be 1573 K for the carbon-reduced iron and 1873 K for the hydrogen-reduced one. Compositions of the liquid slags saturated with *C2S* were determined as given in Table 1 based on the FeO-CaO-SiO_2 ternary phase diagram (Muan and Osborn, 1965), Figure 2, with the assumption that CaO/SiO_2 mole ratios were 2 and mole fractions of P_2O_5 were 0.02. The activities of FeO and P_2O_5 were calculated with a regular solution model (Ban-ya, 1993), and the phosphorus concentrations in the iron could be estimated by solving Equations (2) and (3).

TABLE 1 – Comparison of the phosphorus contents in the C-reduced or H-reduced iron.

Reduced by		Mole fraction in liquid slag				Activity (Ban-ya, 1993)		Mass% content in iron	
	T/K	FeO	CaO	SiO_2	P_2O_5	FeO	P_2O_5	C	P
Carbon	1573	0.73	0.17	0.08	0.02	0.90	6.2×10^{-17}	4.5	0.0024
Hydrogen	1873	0.41	0.38	0.19	0.02	0.55	5.3×10^{-18}	0	0.039

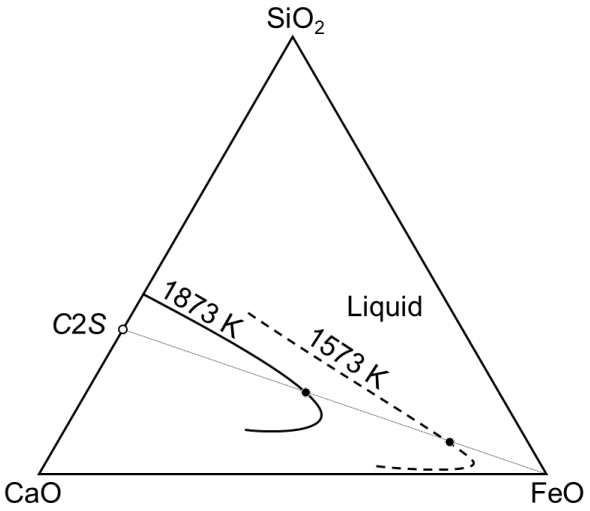

FIG 2 – Schematic phase diagram of the FeO-CaO-SiO_2 ternary system.

The equilibrium phosphorus content in the hydrogen-reduced iron was found to be 16 times higher than that in the carbon-reduced one. In order to overcome such a disadvantageous situation, it is essential to know accurately the basic thermochemical properties of the slags containing <*C*2*S*-*C*3*P*>$_{SS}$.

In the present study, the activities of P_2O_5 were measured in <*C*2*S*-*C*3*P*>$_{SS}$ coexisting with *CS* or CaO through the gas equilibrium method. The P_2O_5 activity depends on not only temperature and the *C*3*P* concentration in <*C*2*S*-*C*3*P*>$_{SS}$ but also the second phase coexisting with the solid solution, *CS* or CaO. Therefore, the thermochemical properties of the solid solution were discussed in terms of the *C*2*S* and *C*3*P* activities, which were determined by only temperature and the composition of <*C*2*S*-*C*3*P*>$_{SS}$. To improve the accuracy of the measurement, the same gas equilibrium method was applied to the MgO-P_2O_5 binary system, in which the P_2O_5 activity has been reported, as a reference system.

EXPERIMENTS

Experimental principle

In the present experiments, liquid Cu-P alloys were brought into equilibrium with MgO + *M*3*P*, <*C*2*S*-*C*3*P*>$_{SS}$ + *CS*, or <*C*2*S*-*C*3*P*>$_{SS}$ + CaO at 1573 K under a stream of Ar + H_2 + H_2O or Ar + H_2 + CO_2 gas mixture, in which the oxygen potential was fixed. The underlying reaction can be expressed as

$$2[P]_{Cu} + (5/2)O_2(gas) = P_2O_{5\ in\ oxide} \quad (4)$$

$$\log K_4 = \log a_{P_2O_5} - 2\log([f_P]_{Cu}\,[mass\%P]_{Cu}) - (5/2)\log(p_{O_2}/atm) \quad (5)$$

It was reported that phosphorus in the molten copper alloy obeyed Henry's law and hence $[f_P]_{Cu}$ was unity in the composition range of $[mass\%P]_{Cu} < 1$ (Iwase, Ichise, and Yamada, 1985). Thus, Equation (5) indicates that K_4 can be determined by analysing the phosphorus content in the copper alloy equilibrated with MgO + *M*3*P*, in which a_{P2O5} is well known, under the fixed oxygen potential. Now that the value for K_4 is available, unknown values for a_{P2O5} in the CaO-SiO_2-P_2O_5 ternary system can

be derived from the phosphorus contents in the copper alloys equilibrated with the ternary oxides under fixed p_{O2}.

Materials and procedure

Regent grade MgO, $Mg(H_2PO_4)_2{\cdot}3H_2O$, $CaCO_3$, and *C3P* were obtained from Nacalai Tesque Inc Kyoto, Japan, while SiO_2 was obtained from Nacalai Tesque Inc Kyoto, Japan and FUJIFILM Wako Pure Chemical Co, Osaka, Japan. A mixture of MgO + $Mg(H_2PO_4)_2{\cdot}3H_2O$ at a mole ratio of 2:1 was heated slowly to 1273 K in air to prepare *M3P*. Lime was obtained by calcining $CaCO_3$ in air at 1373 K. To synthesise *C2S* and *CS*, $CaCO_3$ and SiO_2 were mixed at mole ratios of 2:1 and 1:1, respectively, and heated in air at 1573 K. The resulting compounds were submitted to powder X-ray diffraction analyses to confirm the expected phases only. The obtained *C2S* was mixed with *C3P* and heated at 1573 K to prepare $<C2S\text{-}C3P>_{SS}$. The mole fraction of *C3P* in $<C2S\text{-}C3P>_{SS}$ was 0.20 (31 mass%$Ca_3P_2O_8$). Oxide mixtures of MgO + *M3P*, $<C2S\text{-}C3P>_{SS}$ + *CS*, and $<C2S\text{-}C3P>_{SS}$ + CaO were used for the following experiments. The starting materials for the metallic phase were copper shavings obtained from Nakalai Tesque Inc, Kyoto, Japan and Cu_3P from Hirano Seizaemon Co Ltd, Tokyo, Japan.

Table 2 summarises the experimental conditions. For some conditions, dense alumina crucibles (10 mm od, 8 mm id, and 30 mm in height) were charged with the oxide mixtures and the copper shavings. For the other conditions, the oxide mixtures were pressed in a steel die to form crucible shapes (15 mm od, 8 mm id, and 8 mm in height) and charged with Cu + Cu_3P. The latter is considered a better method that completely prevents contaminations of impurity from crucibles, although little difference was seen in the experimental results described later. Subsequently, the oxide and metallic samples were held at 1573 K in a mullite reaction tube equipped with a SiC resistance furnace, and then the metallic phase melted to form the Cu-P molten alloys coexisting with the oxides. A decomposition reaction of the mullite, $Al_6Si_2O_{13}$, under the reducing atmosphere is expressed as Reaction (6) (Davis. Aksay, and Pask, 1972). From thermal data for Reaction (6) (Kubaschewski, Alcock, and Spencer, 1993), the mullite tube had satisfactory resistance under the present experimental conditions and would not disturb the gas control.

$$Al_6Si_2O_{13}(solid) = 3Al_2O_3(solid) + 2SiO(gas) + O_2(gas) \quad (6)$$

$$\log K_6 = 2\log(p_{SiO}/atm) + \log(p_{O_2}/atm) = -27.3 \quad \text{at 1573 K} \quad (7)$$

TABLE 2 – Experimental conditions and results at 1573 K.

Oxide Sample	$\log(p_{O_2}/atm)$	Holding time /hour	*[mass%*P*]*$_{Cu}$		
			initial	equilibrium	average
MgO + *M3P*	-11.45	42.0	0	0.0225	0.0248 ± 0.0016
		42.0	0.11	0.0264	
		42.0	0.26	0.0254	
MgO + *M3P*	-11.76	44.2	0	0.0543	0.0539 ± 0.0004
		44.2	0.59	0.0535	
MgO + *M3P*	-12.03	42.3	0	0.0765	0.0731 ± 0.0076
		42.3	0.20	0.0802	
		42.3	0.57	0.0625	
MgO + *M3P*	-12.31	45.6	0	0.154	0.159 ± 0.011
		45.6	0.22	0.149	
		45.6	0.64	0.174	
MgO + *M3P*	-12.60	49.1	0	0.395	0.395 ± 0.001
		49.1	0.68	0.394	

TABLE 2 – Experimental conditions and results at 1573 K. (continued)

Oxide Sample	log(p_{O_2}/atm)	Holding time /hour	*[mass%*P*]*$_{Cu}$		
			initial	equilibrium	average
<*C*2*S*-*C*3*P*>$_{SS}$ + *CS*	-12.90	47.3	0	0.0166	0.0159 ± 0.0028
		90.6	0	0.0203	
		142.2	0	0.0137	
		122.8	0	0.0132	
<*C*2*S*-*C*3*P*>$_{SS}$ + *CS* [a]	-12.94	91.3	0	0.0197	0.0209 ± 0.0021
		139.2	0	0.0224	
		161.9	0	0.0248	
		185.1	0	0.0217	
		207.2	0	0.0194	
		230.5	0	0.0182	
		230.5	0	0.0203	
<*C*2*S*-*C*3*P*>$_{SS}$ + *CS*	-13.45	39.8	0	0.0688	0.0765 ±0.0077
		39.8	0.33	0.0842	
<*C*2*S*-*C*3*P*>$_{SS}$ + CaO	-15.35	7.0	0.024	0.00295	0.00288 ± 0.00012
		23.8	0	0.00272	
		23.8	0.013	0.00304	
		23.8	0.024	0.00282	
<*C*.2*S*-*C*3*P*>$_{SS}$ + CaO [a]	-16.10	640.0	0	0.0604	0.0619 ± 0.0055
		754.0	0	0.0619	
		830.0	0	0.0646	
		846.0	0	0.0487	
		851.0	0	0.0619	
		855.0	0	0.0683	
		869.0	0	0.0639	
		941.0	0	0.0658	

a : the samples were charged in the alumina crucibles.

Into the reaction tube, the Ar + H_2 + H_2O or Ar + H_2 + CO_2 gas mixture was introduced to fix the oxygen potential. The Ar + H_2 + H_2O gas mixture prepared by passing the Ar + 12%H_2 gas mixture through distilled water kept at 283 K-304 K in a thermostat bath was used for the experiments with MgO + *M*3*P*. On the other hand, for <*C*2*S*-*C*3*P*>$_{SS}$ + *CS*, the Ar+H_2+H_2O gas mixture was prepared by passing the Ar + 12%H_2 gas mixture through ether distilled water kept at 278 K or LiCl-saturated water kept at 303 K or 313 K. The partial pressures of H_2O and O_2 in these gas mixtures can be calculated from the following thermal data (Kubaschewski and Alcock, 1979; Takeshita, Hasegawa, and Iwase, 2008).

$$\log(p_{H_2O}/\text{atm}) = 19.732 - 2900/(T_{bath}/\text{K}) - 4.65\log(T_{bath}/\text{K})$$

$$\text{distilled water, } 273\ \text{K} < T_{bath} < 373\ \text{K} \qquad (8)$$

$$\log(p_{H_2O}/\text{atm}) = 5.94 - 2510/(T_{bath}/\text{K})$$

LiCl-saturated water, T_{bath} > 291.5 K (9)

$H_2(gas) + (1/2)\,O_2(gas) = H_2O(gas)$ (10)

$\log K_{10} = -(1/2)\log(p_{O_2}/atm) - \log(p_{H_2}/p_{H_2O}) = 5.32$ at 1573 K (11)

, where T_{bath} is the temperature of the thermostat bath. For the experiments with <*C*2*S*-*C*3*P*>$_{SS}$ + CaO, the much lower oxygen potentials were necessary, and thus the following Ar + H_2 + H_2O and Ar + H_2 + CO_2 gas mixtures were used. The Ar + H_2 + H_2O gas mixture was prepared by passing the Ar + 12%H_2 gas mixture through $C_2H_2O_4$ + $C_2H_2O_4{\cdot}2H_2O$ two-phase mixture kept at 268 K. The water vapour pressure in equilibrium with the $C_2H_2O_4$ + $C_2H_2O_4{\cdot}2H_2O$ is given by (Takeshita, Hasegawa, and Iwase, 2008)

$$\log(p_{H_2O}/atm) = 6.88 - 2810/(T_{bath}/K)$$

$C_2H_2O_4$ + $C_2H_2O_4{\cdot}2H_2O$ two-phase mixture, T_{bath} < 293 K (12)

The value for p_{O_2} in this Ar + H_2 + H_2O gas mixture can be obtained from Equation (11). The Ar + H_2 + CO_2 gas mixture was prepared by mixing Ar + 30%H_2 and Ar + 1%CO_2 gas mixtures. The calculating method for the equilibrium partial pressures of gaseous species has been described elsewhere (Iwahashi *et al*, 2021).

After being held at 1573 K, the phosphorus contents in quenched alloys were determined with ICP-OES. Initial compositions of alloys are also listed in Table 2. Except for several conditions, the alloy samples with different initial phosphorus contents were simultaneously held in the reaction tube. When the phosphorus concentration was higher or lower than the equilibrium value, Reaction (4) proceeded toward the right or left hand, respectively. The phosphorus concentrations in such alloys that matched each other within experimental uncertainties were able to be confirmed as the equilibrium value.

RESULTS AND DISCUSSION

Activity measurements of P_2O_5

A typical relationship between the compositions of copper alloys and duration time for MgO + $Mg_3P_2O_8$ is shown in Figure 3. The phosphorus concentrations in the alloys with different initial compositions agreed well after 42.0 hours, and hence the equilibrium value for *[mass%*P*]*$_{Cu}$ was determined to be 0.0248 ± 0.0016.

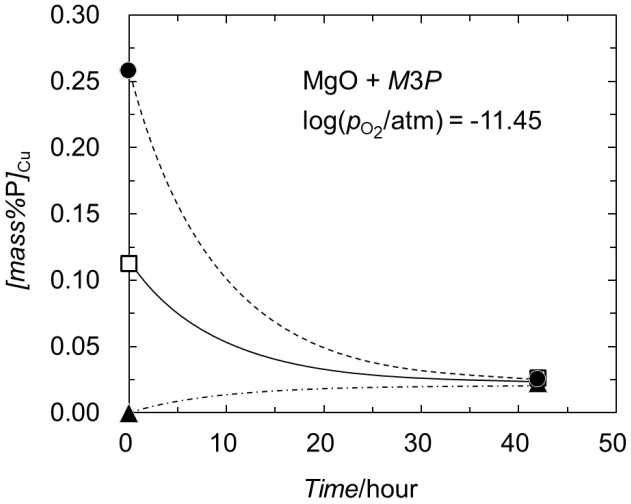

FIG 3 – Typical changes in the compositions of alloys over duration time.

All the experimental results are summarised in Table 2. Equation (13) given by rewriting Eq. (5) indicates that the logarithmic relationship between *[mass%*P*]*$_{Cu}$ and p_{O_2} should be linear with a slope of - 5/4 and an intercept of [- (1/2)logK_4 + (1/2)log$a_{P_2O_5}$].

$$\log[mass\%P]_{Cu} = -(5/4)\log(p_{O_2}/atm) - (1/2)\log K_4 + (1/2)\log a_{P_2O_5} \quad (13)$$

Figure 4 shows such relationships. Linear relations can be observed for the three types of oxide mixtures and their slopes are close to - 5/4.

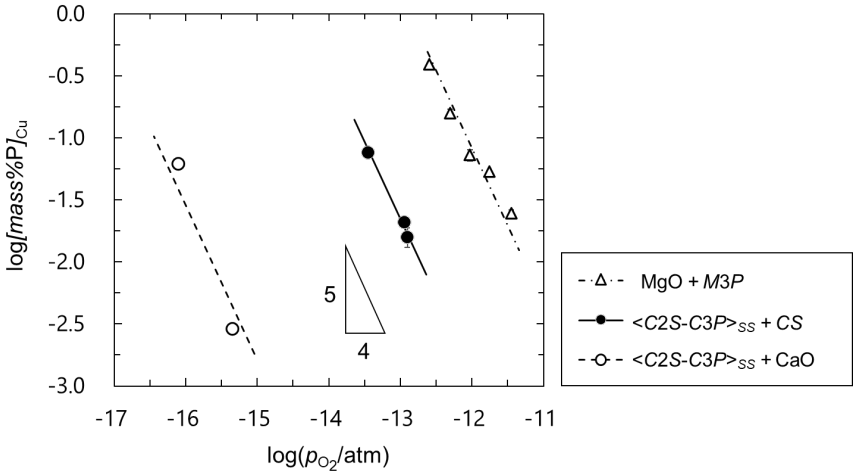

FIG 4 – Relationship between log*[mass%*P*]*$_{Cu}$ and log(p_{O_2}/atm) at 1573 K.

The P_2O_5 activity in the MgO + *M*3*P* two-phase mixture at 1573 K can be derived from the following formulae (Pandit and Jacob, 1995; Jung and Hudon, 2012).

$$3\,\mathrm{MgO(solid)} + P_2O_{5\ \text{in}\ M3P} = M3P\text{(solid)} \quad (14)$$

$$\log K_{14} = -\log a_{P_2O_5(\mathrm{MgO}+M3P)} = 13.6 \quad \text{at 1573 K} \quad (15)$$

From Equation (13), K_4 was determined from the intercept of the regression line for MgO + *M*3*P* in Figure 4.

$$\log K_4 = -18.5 \pm 0.2 \quad \text{at 1573 K} \quad (16)$$

By using the obtained value for K_4, the P_2O_5 activity in <*C*2*S*-*C*3*P*>$_{SS}$ coexisting with *CS* or CaO at 1573 K was determined from the intercept of the regression line for the corresponding oxide mixture in Figure 4.

$$\log a_{P_2O_5(<C2S\text{-}C3P>_{SS}+CS)} = -17.3 \pm 0.1 \quad \text{at 1573 K} \quad (17)$$

$$\log a_{P_2O_5(<C2S\text{-}C3P>_{SS}+\mathrm{CaO})} = -24.5 \pm 0.4 \quad \text{at 1573 K} \quad (18)$$

The P_2O_5 activity in <*C*2*S*-*C*3*P*>$_{SS}$ + CaO was found to be about seven digits lower than that in <*C*2*S*-*C*3*P*>$_{SS}$ + *CS* even at the same composition of <*C*2*S*-*C*3*P*>$_{SS}$, 31 mass%*C*3*P*.

The activities of Ca_2SiO_4, $Ca_{1.5}PO_4$, CaO, and SiO_2 in the solid solution

The simple CaO-SiO_2 binary system is focused on at the beginning of this section. Figure 5 gives the CaO and SiO_2 activities against the composition in the binary system at 1573 K calculated by thermal data (Kubaschewski, Alcock, and Spencer, 1993; Seetharaman, 2014) as well as assessed results by CALPHAD approach in the latest study (Abdul *et al*, 2023). Both values are in good agreement. As shown in this figure, the activities of components change drastically within the quite narrow composition ranges of the stoichiometric compounds ($CaSiO_3$, $Ca_3Si_2O_7$, Ca_2SiO_4, and Ca_3SiO_5). For example, at the composition of *CS*, the activity of *CS* is unity and hence a product of a_{CaO} and a_{SiO_2} is fixed by Equation (19).

$$\mathrm{CaO}_{\ \text{in}\ CS} + \mathrm{SiO_{2\ in}}_{\ CS} = CS\text{(solid)} \quad (19)$$

$$\log K_{19} = -\log(a_{CaO}\, a_{SiO_2}) = 2.92 \quad (20)$$

Nevertheless, each value for the CaO and SiO_2 activities in *CS* cannot be determined as shown in Figure 5.

$$-2.92 < \log a_{CaO(CS)} < -2.07 \quad \text{at 1573 K} \quad (21)$$

$$-0.85 < \log a_{SiO_2(CS)} < 0 \quad \text{at 1573 K} \quad (22)$$

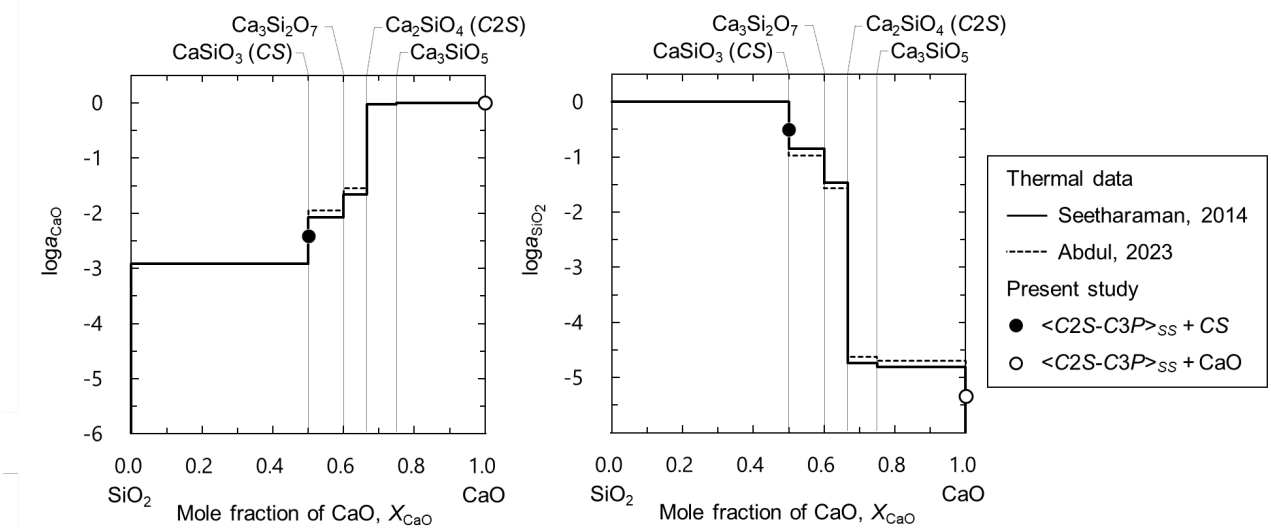

FIG 5 – Activities of components in the CaO-SiO_2 binary system at 1573 K.

Similarly, the *C*2*S* and *C*3*P* activities are determined depending on temperature and the composition of <*C*2*S*-*C*3*P*>$_{SS}$, while the P_2O_5 activity depends not only on these variables but also on the second phase coexisting with <*C*2*S*-*C*3*P*>$_{SS}$. In the <*C*2*S*-*C*3*P*>$_{SS}$ + *CS* and <*C*2*S*-*C*3*P*>$_{SS}$ + CaO two-phase regions, Reactions (23) and (25) achieve the equilibrium states, respectively, and hence the P_2O_5 activities are determined through the *C*2*S* and *C*3*P* activities.

$$P_2O_{5\ in\ SS} + 3\,C2S_{\ in\ SS} = C3P_{\ in\ SS} + 3\,CS(\text{solid}) \quad (23)$$

$$\log K_{23} = \log a_{C3P} - 3\log a_{C2S} - \log a_{P_2O_5(<C2S\text{-}C3P>_{SS}+CS)} = 16.50 \quad \text{at 1573 K}$$

(Kubaschewski, Alcock, and Spencer, 1993; Seetharaman, 2014) (24)

$$P_2O_{5\ in\ SS} + 3\,CaO(\text{solid}) = C3P_{\ in\ SS} \quad (25)$$

$$\log K_{25} = \log a_{C3P} - \log a_{P_2O_5(<C2S\text{-}C3P>_{SS}+CaO)} = 21.99 \quad \text{at 1573 K}$$

(Jung and Hudon, 2012; Hudon and Jung, 2015) (26)

Therefore, the *C*2*S* and *C*3*P* activities should be considered in order to understand the thermochemical properties of the solid solution. From the experimental results, the *C*3*P* activity can be obtained by Equations (18) and (26).

$$\log a_{C3P} = -2.54 \quad (27)$$

In addition, the *C*2*S* activity can be derived by Equations (17), (24), and (27).

$$\log a_{C2S} = -0.59 \quad (28)$$

The standard states of a_{C3P} and a_{C2S} were taken to be pure supercooled solid *ά*-*C*3*P* and *α*-*C*2*S*, respectively. In the solid solutions, the anion SiO_4^{4-} is thought to be replaced by PO_4^{3-} (Suzuki, Umesaki, and Ishii, 2022). Although tri-calcium phosphate has conventionally been treated as $Ca_3P_2O_8$, it should be better to consider the chemical compound containing a single PO_4^{3-}, ie, $Ca_{1.5}PO_4$ (= (1/2)*C*3*P*); the relationship between the activities of $Ca_{1.5}PO_4$ and $Ca_3P_2O_8$ can be formulated as

$$\log a_{(1/2)C3P} = (1/2)\log a_{C3P} = -1.327 \quad (29)$$

Figure 6 shows the activities of (1/2)*C*3*P* and *C*2*S* plotted against the mole fraction of (1/2)*C*3*P*, $X_{(1/2)C3P}$, in the *C*2*S*-(1/2)*C*3*P* binary system. The curves in this figure represent calculated values from a sub-regular solution model, Equation (30) and (31). The parameters, *A* and *B*, were determined based on the present results.

$$\log a_{(1/2)C3P} = \log X_{(1/2)C3P} + A(1 - X_{(1/2)C3P})^3 + B(1 - X_{(1/2)C3P})^2 \quad (30)$$

$$\log a_{C2S} = \log(1 - X_{(1/2)C3P}) - AX_{(1/2)C3P}{}^3 + (1.5A + B)X_{(1/2)C3P}{}^2 \quad (31)$$

$$A = -3.89 \quad (32)$$

$$B = 0.81 \quad (33)$$

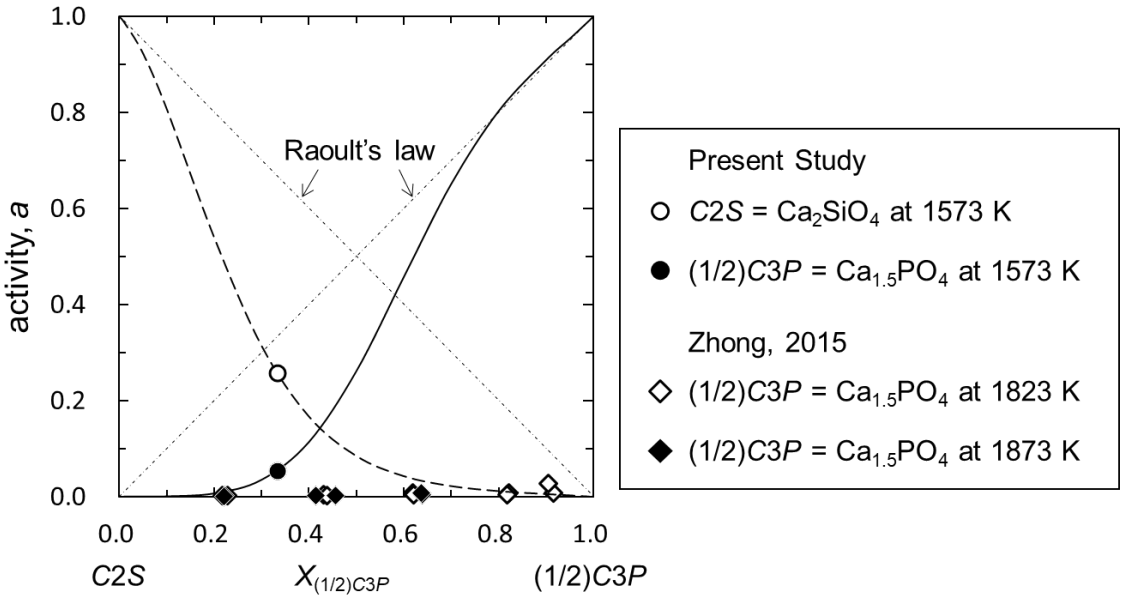

FIG 6 – Activities of components in the Ca_2SiO_4-$Ca_{1.5}PO_4$ binary system.

Figure 6 also shows literature data at higher temperatures, in which the P_2O_5 and *C*3*P* activities have been measured in <*C*2*S*-*C*3*P*>$_{SS}$ + CaO at 1823 K and 1873 K (Zhong, Matsuura, and Tsukihashi, 2015). Although the activities of (1/2)*C*3*P* at higher temperatures were much lower than the present result, the activities of components in this system exhibited large negative deviations from Raoult's law. It implies the strong chemical affinity between SiO_4^{4-} and PO_4^{3-} in the solid solution, which is consistent with the fact that *C*2*S* can incorporate *C*3*P* in the whole composition range as shown in Figure 1b.

Once the thermochemical properties of <*C*2*S*-*C*3*P*>$_{SS}$ are clarified, the CaO and SiO_2 activities can be calculated in the solid solutions coexisting with *CS* or CaO from the following reactions.

<*C*2*S*-*C*3*P*>$_{SS}$ + *CS* two-phase region

$$CaO_{\text{ in } SS} + CS(\text{solid}) = C2S_{\text{ in } SS} \quad (34)$$

$$\log a_{CaO(<C2S\text{-}C3P>_{SS}+CS)} = -\log K_{34} + \log a_{C2S} = -2.42 \quad \text{at 1573 K} \quad (35)$$

$$SiO_{2\text{ in } SS} + C2S_{\text{ in } SS} = 2\,CS(\text{solid}) \quad (36)$$

$$\log a_{SiO_2(<C2S\text{-}C3P>_{SS}+CS)} = -\log K_{36} - \log a_{C2S} = -0.50 \quad \text{at 1573 K} \quad (37)$$

<*C*2*S*-*C*3*P*>$_{SS}$ + CaO two-phase region

$$2CaO(\text{solid}) + SiO_{2\text{ in } SS} = C2S_{\text{ in } SS} \quad (38)$$

$$\log a_{CaO(<C2S\text{-}C3P>_{SS}+CaO)} = 0 \quad (39)$$

$$\log a_{SiO_2(<C2S\text{-}C3P>_{SS}+CaO)} = -\log K_{38} + \log a_{C2S} = -5.34 \quad \text{at 1573 K} \quad (40)$$

The values for K_{34}, K_{36}, and K_{38} were obtainable from the thermal data (Kubaschewski, Alcock, and Spencer, 1993; Seetharaman, 2014). The calculated results are superimposed in Figure 5. The calculated result of the CaO and SiO_2 activities in the presence of *CS*, Equations (35) and (37), were within the activity ranges (21) and (22), respectively. It can be said that the present results are not inconsistent with the literature data for the CaO-SiO_2 binary system.

Experimental error in the gas equilibrium method

The gas equilibrium method, in which the Cu-P liquid alloys are equilibrated with oxides, has been pointed out to involve relatively large experimental errors in analysing the compositions of the copper alloys because of the very low phosphorus contents in the alloys (Yamasue, Shimizu, and Nagata, 2013). Such experimental errors are discussed in the last section. The equilibrium constants

of Reaction (4) in the experiment for MgO + *M*3*P*, <*C*2*S*-*C*3*P*>$_{SS}$ + *CS*, and <*C*2*S*-*C*3*P*>$_{SS}$ + CaO are expressed as

$$\log K_4 = \log a_{P_2O_5(MgO+M3P)} - 2\log [mass\%P]_{Cu} - (5/2)\log(p_{O2(MgO+M3P)}/atm) \quad (41)$$

$$\log K_4 = \log a_{P_2O_5(<C2S\text{-}C3P>_{SS}+CS)} - 2\log [mass\%P]_{Cu} - (5/2)\log(p_{O_2(<C2S\text{-}C3P>_{SS}+CS)}/atm) \quad (42)$$

$$\log K_4 = \log a_{P_2O_5(<C2S\text{-}C3P>_{SS}+CaO)} - 2\log [mass\%P]_{Cu} - (5/2)\log(p_{O_2(<C2S\text{-}C3P>_{SS}+CaO)}/atm) \quad (43)$$

When the three regression lines in Figure 4 are compared with a fixed value for $\log [mass\%P]_{Cu}$ on the vertical axis, the differences between Equations (41) and (42) or (43) are written as

$$\log a_{P_2O_5(<C2S\text{-}C3P>_{SS}+CS)} = \log a_{P_2O_5(MgO+M3P)} + (5/2)\log(p_{O_2(<C2S\text{-}C3P>_{SS}+CS)}/p_{O_2(MgO+M3P)}) \quad (44)$$

$$\log a_{P_2O_5(<C2S\text{-}C3P>_{SS}+CaO)} = \log a_{P_2O_5(MgO+M3P)} + (5/2)\log(p_{O_2(<C2S\text{-}C3P>_{SS}+CaO)}/p_{O_2(MgO+M3P)}) \quad (45)$$

Equations (44) and (45) indicate that the P_2O_5 activities in <*C*2*S*-*C*3*P*>$_{SS}$ + *CS* and <*C*2*S*-*C*3*P*>$_{SS}$ + CaO can be derived from the ratios of $p_{O_2(<C2S\text{-}C3P>_{SS}+CS)}$ and $p_{O_2(<C2S\text{-}C3P>_{SS}+CaO)}$ against $p_{O_2(MgO+M3P)}$. In other words, the experimental errors in analysing the alloy compositions would be cancelled out in calculating $a_{P_2O_5}$ since they would be involved in all the experimental procedures for MgO + *M*3*P*, <*C*2*S*-*C*3*P*>$_{SS}$ + *CS*, and <*C*2*S*-*C*3*P*>$_{SS}$ + CaO, which makes the present results more reliable.

CONCLUSIONS

For a better understanding of the dephosphorization reaction in the steelmaking process, the present study focused on the thermochemical properties of the oxides containing the Ca_2SiO_4-$Ca_3P_2O_8$ solid solutions, <*C*2*S*-*C*3*P*>$_{SS}$. The P_2O_5 activities were measured in the solid solution coexisting with $CaSiO_3$ or CaO through the gas equilibrium method, in which the Cu-P liquid alloys were brought into equilibrium with the oxides under fixed oxygen potentials at 1573 K.

$$2\,[P]_{Cu} + (5/2)\,O_2(gas) = P_2O_5$$

$$\log a_{P_2O_5(MgO+M3P)} = 2\log [mass\%P]_{Cu} + (5/2)\log(p_{O_2}/atm) + \log K$$

The value for *K* was determined by the same experimental method applied to the MgO + $Mg_3P_2O_8$ two-phase mixture, in which the P_2O_5 activity was well known. The obtained results at 1573 K are summarised as follows.

$$\log K = -18.5 \pm 0.2$$

$$\log a_{P_2O_5(<C2S\text{-}C3P>_{SS}+CaSiO_3)} = -17.3 \pm 0.1$$

$$\log a_{P_2O_5(<C2S\text{-}C3P>_{SS}+CaO)} = -24.5 \pm 0.4$$

, where *C*3*P* contents are 31 mass% in <*C*2*S*-*C*3*P*>$_{SS}$. The P_2O_5 activity in <*C*2*S*-*C*3*P*>$_{SS}$ + CaO was found to be about seven digits lower than that in <*C*2*S*-*C*3*P*>$_{SS}$ + $CaSiO_3$. The experimental results can be understood in terms of the activities of Ca_2SiO_4 and $Ca_{1.5}PO_4$ (= (1/2)$Ca_3P_2O_8$). The activities of components in the Ca_2SiO_4-$Ca_{1.5}PO_4$ binary system exhibited negative deviations from Raoult's law, indicating the strong chemical affinity between the components in the solid solutions.

ACKNOWLEDGEMENTS

This work was supported by JSPS KAKENHI Grant Number 22KJ1689 and 21K04737. Experimental assistance was provided by Mr. Taihei SAITO, Graduate Student, Department of Energy Science and Technology, Kyoto University, Mr. Toru NISHIMURA, Graduate Student, Department of Energy Science and Technology, Kyoto University, and Ryunosuke KONDO, Undergraduate Student, Faculty of Engineering, Kyoto University. These are gratefully acknowledged.

REFERENCES

Abdul, W, Mawalala, C, Pisch, A and Bannerman, M, N, 2023. CaO-SiO2 assessment using 3rd generation CALPHAD models, in *Cement and Concrete Research*, 173, p. 107309. https://doi.org/10.1016/j.cemconres.2023.107309

Ban-ya, S, 1993. Mathematical expression of slag-metal reactions in steelmaking process by quadratic formalism based on the regular solution model, in *ISIJ international*, 33, pp 2-11. https://doi.org/10.2355/isijinternational.33.2

Davis, R, F, Aksay, I, A, and Pask, J, A, 1972. Decomposition of mullite, in *Journal of the American Ceramic Society*, 55, pp 98-101. https://doi.org/10.1111/j.1151-2916.1972.tb11218.x

Fix, W, Heymann, H, and Heinke, R, 1969. Subsolidus relations in the system 2CaO·SiO2-3CaO·P2O5, in *Journal of the American Ceramic Society*, 52, pp 346-347.

Hino, M and Ito, K, 2009. Thermodynamic Data for Steelmaking, p 30, p 251, p 259 (Tohoku University Press, Sendai).

Hudon, P and Jung, I, 2015. Critical Evaluation and Thermodynamic Optimization of the CaO-P2O5 System, in *Metallurgical and Materials Transactions B*, 46, pp 494–522. https://doi.org/10.1007/s11663-014-0193-x

Iwahashi, K, Hashimoto, S., Yamauchi, R, Saito, K, and Hasegawa, M, 2021. Phase relationship and activities of components in CaO-SiO2-Cr2O3 ternary system at 1573 K, in *ISIJ International*, 61, pp 1404–1411. https://doi.org/10.2355/ISIJINTERNATIONAL.ISIJINT-2020-752

Iwase, M, Ichise, E and Yamada, N, 1985. Activities of phosphorus in liquid copper by solid oxide galvanic cell, in *Steel Research*, 56, pp 319-326. https://doi.org/10.1002/srin.198500642

Jung, I, and Hudon, P, 2012. Thermodynamic assessment of P2O5, in *Journal of the American Ceramic Society*, 95, pp 3665–3672. https://doi.org/10.1111/j.1551-2916.2012.05382.x

Kashiwaya, Y, and Hasegawa, M, 2012. Thermodynamics of impurities in pure iron obtained by hydrogen reduction, in *ISIJ International*, 52, pp 1513–1522. https://doi.org/10.2355/isijinternational.52.1513

Kitamura, S, Shibata, H and Maruoka, N, 2008. Kinetic Model of Hot Metal Dephosphorization by Liquid and Solid Coexisting Slags, in *Steel Research International*, 79, pp 586-590. https://doi.org/10.1002/srin.200806170

Kubaschewski, O and Alcock, C, B, 1979. Metallurgical Thermochemistry, 5th edition, pp 358-384 (Pergamon Press, Oxford: UK).

Kubaschewski, O, Alcock, C, B, and Spencer, P, J, 1993. Materials Thermochemistry, 6th edition, pp 257-323 (Pergamon Press, Oxford: UK).

Matsu-suye, M, Hasegawa, M, Fushi-tani, K, and Iwase, M, 2007. Phase Equilibrium of the System CaO-P2O5-SiO2 between 1473 K and 1673 K, in *Steel Research International*, 78, pp 465-467. https://doi.org/10.1002/srin.2007062323

Muan, A and Osborn, E, F, 1965. Phase Equilibria among Oxides in Steelmaking, p 113 (Addison- Wesley Publishing Company, Reading, MA)

Pandit, S, S, and Jacob, K, T, 1995. Thermodynamic Properties of Magnesium Phosphate (Mg3P2O8) Correction of Data in Recent Compilations, in *Metallurgical and Material Transactions A*, 26, pp 225-227. https://doi.org/10.1007/BF02669808

Seetharaman, S, 2014. Treatise of Process Metallurgy Vol 1 Process Fundamentals, pp 527-556 (Elsevier, Oxford).

Suzuki, M, Umesaki, N, and Ishii, Y, 2022. Highly disordered ionic distribution in α-dicalcium silicate for structure relaxation, in *Journal of the American Ceramic Society*, 105, pp 700–711. https://doi.org/10.1111/jace.18096

Takeshita, H, Hasegawa, M, and Iwase, M, 2008. Water Vapor Pressures of LiCl-2H2O-Saturated Solutions and C2H2O4-2H2O-C2H2O4 Mixtures, in *High Temperature Materials and Processes*, 27, pp. 19-22. https://doi.org/10.1515/HTMP.2008.27.1.19

Uchida, Y, Watanabe, C, and Hasegawa, M, 2021. Phase Equilibria in High Phosphate-Containing Slag without CaO Saturation at Elevated Temperature, in *Tetsu-to-Hagané*, 107, pp 701-707. https://doi.org/10.2355/tetsutohagane.TETSU-2021-046

Uchida, Y, Watanabe, C, and Tsuruoka, H, 2022. Basic Evaluation of Phase Relation in a Phosphorus-Containing System Saturated with CaSiO3 at Elevated Temperatures for the Utilization of Steelmaking Slag and Sewage Sludge as Phosphorus Resources, in *Minerals*, 12, p 266. https://doi.org/10.3390/min12020266

Yamasue, E, Shimizu, K, and Nagata, K, 2013. Direct determination of standard Gibbs energies of the formation of 4CaO·P2O5 and 3CaO·P2O5 by transpiration method, in *ISIJ International*, 53, pp 1828–1835. https://doi.org/10.2355/isijinternational.53.1828

Zhong, M, Matsuura, H, and Tsukihashi, F, 2015. Activity of phosphorus pent-oxide and tri-calcium phosphate in 2CaO·SiO2-3CaO·P2O5 solid solution saturated with CaO, in *Materials Transactions B*, 56, pp 1192–1198. https://doi.org/10.2320/matertrans.M-M2015813